JETIR.ORG ISSN: 2349-5162 | ESTD Year : 2014 | Monthly Issue
JOURNAL OF EMERGING TECHNOLOGIES AND INNOVATIVE RESEARCH (JETIR)
An International Scholarly Open Access, Peer-reviewed, Refereed Journal

PREFERENTIAL ANTICANCER ACTIVITY OF BIOGENIC SELENIUM NANOPARTICLES FROM *VACCINIUM* SECT. *CYANOCOCCUS* FRUIT EXTRACT

[1]Godithala Pardha Saradhi, [1]Usha Kiranmayi Mangamuri, *[1]Sudhakar Poda

[1]Department of Biotechnology, Acharya Nagarjuna University, Guntur – 522 510, Andhra Pradesh, India.

*** Corresponding author:**

Dr. Sudhakar Poda. *Assistant professor, Department of Biotechnology, Acharya Nagarjuna University, Guntur – 522 510, Andhra Pradesh, India.* E-mail Id: sudhakarpodha@gmail.com

Abstract:

The study examined the role of *Vaccinium* sect. *Cyanococcus* fruit extract as reducing and stabilizing agents in the biosynthesis of selenium nanoparticles (Bgn-SeNPs) and followed by focused on the assessment of preferential anticancer effects of Bgn-SeNPs. *Vaccinium* sect. *Cyanococcus* (VC) fruits were purchased from a nearby market in Vijayawada, Andhra Pradesh. The cold maceration technique was chosen oven Soxhlet extraction technique to obtain VC fruit extract. The biosynthesis of selenium nanoparticles (Bgn-SeNPs) was carried out using *Vaccinium* sect. *Cyanococcus* (VC) fruit extract as reducing and stabilizing agent. As-synthesized biogenic selenium nanoparticles (Bgn-SeNPs) were subjected to various physico-chemical characterization analyses by various nanotechnological approaches. UV-Visible spectroscopy absorbance peak for Bgn-SeNPs was noticed at 320 nm. XRD analysis revealed that Bgn-SeNPs was not exhibited crystalline nature and were found to have amorphous in nature. DLS pattern showed that Bgn-SeNPs were in the range of nano-sized, with an average size of 130 nm. Zeta potential analysis showed that Bgn-SeNPs were highly stable with a charge of -25 mV. SEM analysis showed that Bgn-SeNPs were irregular in shape, had a slight aggregation, and had a size range between 106 – 150 nm. Following, study focused on the assessment of preferential anticancer effects of Bgn-SeNPs and it was evaluated by related to toxicity towards normal cells by MTT, LDH, and micro-morphological assessments. Anticancer activity of Bgn-SeNPs was performed on various cancer cell line models, which include RAW 264.7 (mouse macrophage cells), A549 (human lung cancer cells), MDA-MB-231 (human breast cancer cells), and Caco-2 (human intestinal cells). The biocompatibility of Bgn-SeNPs was evaluated by the accomplishment of the cytotoxicity analysis on human normal kidney cells HEK-293. MTT assay showed that Bgn-SeNPs have dose-dependent effect on viability of cancer and normal cells. In MTT assay, IC_{50} values of Bgn-SeNPs (concentration required to inhibit 50% of cell viability) on RAW 264.7, A549, MDA-MB-231, and Caco-2 cancer cells were determined as 64.29 ± 3.71, 38.03 ± 2.14, 67.81 ± 3.05, and 54.73 ± 2.90 µg/mL, respectively. The Bgn-SeNPs have exhibited superior anticancer activity on A549 cells. In the LDH assay, superior LDH release was noticed in cancer cells at lower concentrations of Bgn-SeNPs. Whereas, Bgn-SeNPs induced the LDH release in normal at a higher dosage. The anticancer and cytotoxic effect of Bgn-SeNPs on cancer and normal cells were revealed by micro-morphological observation. The dose of Bgn-SeNPs required to induce detrimental changes in the micro-morphology of normal was quite higher related to cancer cells. The study concluded that as-synthesized Bgn-SeNPs were highly selective in inhibiting the cancer cells in relation to normal cells.

Key words: Selenium nanoparticles, *Vaccinium* sect. *Cyanococcus*, UV-Visible spectroscopy, Scanning electron microscope, Anticancer activity, MTT assay, LDH assay, Micro-morphological observation.

I. Introduction

Nanotechnology is a new revolution with enormous potential across a wide range of industries, from mechanics to healthcare (Koshovets & Ganichev, 2017). It is the study of manipulating and controlling matter on an atomic and molecular scale with at least one distinctive dimension in the nanometer range, often between 1 and 100 nm. It works with nanoscale materials and can develop new tools and methods. It is thought that a nanoparticle is a tiny object that works as a single entity, has distinct traits and functions, and establishes a new level of activity. In comparison to larger particles, nanoparticles appear to have higher levels of chemical and biological activity, enzymatic reactivity, penetrability, catalytic behavior, and quantum characteristics due to their increased surface area and mass transfer rates (with the same composition) (Roduner, 2006).

Nanoparticles (nanoparticles) have drawn a lot of interest in biological applications due to their distinctive physicochemical characteristics (Habeeb Rahuman et al., 2022). In the field of medicine, metal- and metal oxide-supported nanomaterials have demonstrated considerable therapeutic efficacy. To establish its significance and to enhance its activity in health and medicinal applications, the mechanisms relating to the interaction of nanoparticles with animal and plant cells can be utilized. Silver, gold, copper, iron, zinc, selenium, platinum, and other metal-based nanoparticles have attracted a lot of interest in medicine. Metal nanoparticles have been employed in a variety of biological applications, including gene transport, anticancer treatment, radiation enhancement, medication administration, thermal ablation, antibacterial treatment, diagnostic assays, and many others (Yaqoob et al., 2020).

Selenium nanoparticles (SeNPs) have benefits over other nanomaterials. According to reports, selenium is a crucial element that serves as a cofactor and coenzyme at the catalytically active sites of a number of selenoproteins and enzymes in the human body. It also protects cells and tissues from oxidative stress and damage. Along with having pharmacological value, the usage of SeNPs and their supplements helps to strengthen and get the body's immune system ready to fight viruses (Akram et al., 2020). Unfortunately, a high selenium intake can also lead to a number of fatal conditions. Controlling the therapeutic dose is crucial since the toxicity and activity of selenium are typically influenced by large doses (He et al., 2018). Physical, chemical, and biological synthesis techniques can be used to create SeNPs (Khanna et al., 2022). Utilizing a variety of dangerous chemicals to convert sodium selenite salt (Na_2SeO_3) into Se° is a necessary step in the chemical manufacture of nanomaterials. However, the cost-ineffectiveness and significant environmental biosafety and toxicity problems have led to a rising intolerance for the physical and chemical methods of nanoparticle manufacturing. The biosynthesis of SeNPs has been suggested as a feasible conventional alternative technique to deal with these problems. In the biological synthesis, living organisms like plants, algae, fungi, and bacteria are used in the manufacture of SeNPs (Wadhwani et al., 2016). Among biosynthetic methods, plant-based synthesis of SeNPs has advantages over regular or traditional synthesis processes due to their sound biomedical nature. An economical and environmentally beneficial method for synthesizing SeNPs is to use plants as the stabilizing and reducing agents. Beginning in the early 20th century, plant extracts were used to facilitate the synthesis of nanoparticles, and the ability of several plant species to reduce and stabilize SeNPs has since been investigated (Ikram et al., 2021).

This study examined the role of *Vaccinium* sect. *Cyanococcus* fruit extract phytochemicals as reducing and stabilizing agents in the synthesis of selenium nanoparticles (SeNPs). The nanotechnological properties of the biogenic SeNPs (Bgn-SeNPs) were determined by UV-visible absorbance, size distribution, charge, nature, shape, and size. Following, study focused on the assessment of preferential anticancer effects of Bgn-SeNPs and it was evaluated by related to toxicity towards normal cells.

II. Materials and methods

2.1 Chemicals and reagents

Fetal bovine serum (FBS), (3-(4,5-dimethylthiazol-2-yl)-2,5-diphenyltetrazolium bromide (MTT), dichlorohydrofluorescein diacetate (DCFH-DA), rhodamine 123, 4′,6-diamidino-2-phenylindole (DAPI), and Mueller Hinton media were supplied by HiMedia, Mumbai, India. Lactate dehydrogenase (LDH) and malondialdehyde (MDA) assay kits were received from Agappe Diagnostics, Bengaluru, India. Sodium selenite (99.99%), Dulbecco's modified Eagle's medium (DMEM), trypsin, 0.22 µm syringe filter, amphotericin B, penicillin, streptomycin, Dulbecco's phosphate-buffered saline (DPBS), water (HPLC grade), Whatman no.1 filter papers, and Caspase-3 assay kit were procured from Sigma-Aldrich, Bengaluru, India. Tween 80, ethanol (99.99%), methyl alcohol, acetonitrile, dimethyl sulfoxide (DMSO), and other chemicals of satisfactory/fine ranking were attained as of Merck Millipore Corporation, Bengaluru, India.

2.2 Collection and preparation of *Vaccinium* sect. *Cyanococcus* fruit extract

Vaccinium sect. *Cyanococcus* fruits were obtained from fruit market, Vijayawada, Andhra Pradesh. The dust and dirt were removed by washing with double distilled water. The fruits were dried under shade and sliced in an electrical chopper to fine powder. The *Vaccinium* sect. *Cyanococcus* fruit extract was prepared by dissolving powder (10 g) in 100 mL of ethanol and followed by cold maceration method. The obtained fruit extract powder was stored at 4° C and used for nanoparticles synthesis.

2.3 Biogenic synthesis of selenium nanoparticles

To make sodium selenite solution, a 1 M stock solution was prepared in 50 mL, and from that standard stock solution, 50 mM dilution was made, which had been utilized to make nanoparticles. In the same beaker, a 50 mM sodium selenite solution was combined with *Vaccinium* sect. *Cyanococcus* fruit extract. The mixture was then agitated for 1,500 – 1,800 sec on a magnetic stirrer to achieve homogeneity. The pH was regulated to 7, which is neutral using 1 N HCl and 0.5 N NaOH. It was then shaken for 3 hrs at 200 rpm in an orbital shaker at 70 °C in the dark. After 3 hrs, the sample mixture showed a small color change, and the temperature was dropped to 37 °C for 72 hrs. In the solution, a significant color change from pale yellow to brick red was noted after 3 days. The sample tubes then were transferred from the shaker to the incubator and kept at the same temperature. The biogenic selenium nanoparticles (Bgn-SeNPs) were collected near the base of the falcon tube after the other 2 – 3 days of incubation. The collected Bgn-SeNPs were dried at 45 °C and crushed to a fine powder using a mortar and pestle (Alvi et al., 2021).

2.4 Physiochemical characterization of Bgn-SeNPs

The physico-chemical properties of Bgn-SeNPs were determined by ultraviolet-visible spectroscopy, X-ray diffractometry, dynamic light scattering particle size, zeta potential, and scanning electron microscope analysis.

2.5 Anticancer activity of Bgn-SeNPs

2.5.1 Experimental design

Anticancer activity of Bgn-SeNPs was performed on various cancer cell line models, which include RAW 264.7 (mouse macrophage cells), A549 (human lung cancer cells), MDA-MB-231 (human breast cancer cells), and Caco-2 (human intestinal cancer). The biocompatibility of Bgn-SeNPs was evaluated by the accomplishment of the cytotoxicity analysis on human normal kidney cells HEK-293. Cell viability assays (MTT, LDH, and micro-morphological observation tests) were used to measure the anticancer activity of Bgn-SeNPs on cancer cells (RAW 264.7, A549, MDA-MB-231, and Caco-2).

2.5.2 Cell culture and maintenance

The cells were obtained from the National Centre for Cell Science (NCCS) in Pune, India, and were grown in T-75 flasks and T-25 flasks as adherent cultures at 37 °C in DMEM medium enriched with 10% FBS, 2 mM L-glutamine, 100 units/mL of penicillin, and 100 µg/mL of streptomycin in a humid environment usually contains 5% CO_2. Cells were trypsinized (0.25 % trypsin and 0.1 % EDTA), centrifuged (Remi, India), and suspended in DMEM media once they achieved 80% confluence (typically after 2 to 3 days of incubation). The cells which exhibited more than 95% vitality were used for the assays. The cells were seeded in plates, coverslips, and 60 mm Petri dishes in DMEM without FBS for experimental investigations.

2.5.3 Cell viability analysis of Bgn-SeNPs

2.5.3.1 MTT assay

With a few minor adjustments from the method previously reported by Venkatesan et al. (2019), the effect of Bgn-SeNPs on the cell viability of both cancer cells and normal cells was assessed. Briefly, cells in the exponential growth phase were seeded in 96-well flat-bottom culture plates at a density of 1.5×10^4 cells per well in a 0.1 mL DMEM complete medium. For 12 hours, the cells were allowed to adhere and develop in an incubator at 37 °C. Following that, DMEM media was aspirated and replaced with 0.1 mL of fresh, FBS-free DMEM medium containing different doses of Bgn-SeNPs dispersion. The control cells were treated with equivalent volumes of DMEM media without Bgn-SeNPs. Following 24 hrs of the incubation period, the culture medium was removed, thereafter 30 µL of filtered MTT solution (5 mg/mL) in PBS (pH 7.4) was added to each well. After 4 hrs of incubation, MTT solution was replaced with DMSO (100 µL) to dissolve the purple formazan crystals which were reduced from MTT by active mitochondria of viable cells. Plates were shaken, and a microplate reader was used to detect the formazan dye's optical density spectrophotometrically at 570 nm (Synergy H1, BioTek, USA) (Vundela et al., 2022). The assay was carried out three times. The percentage of cell viability compared to the untreated control cells (% of control) was used to express the cytotoxic effect of each treatment:

$$\text{Cell proliferation (\% of control)} = [[OD_{570\ nm} \text{ treated cells}]/[OD_{570\ nm} \text{ control cells}]] \times 100.$$

2.5.3.2 Lactate dehydrogenase release assay

Briefly, cells at a density of $5x10^5$ were seeded in wells of 12-well plates in DMEM complete medium (containing 10% FBS) and allowed to adhere for 12 hrs. Following DMEM complete media was replaced with DMEM incomplete media (without FBS) containing different concentrations of Bgn-SeNPs and incubated for 24 hrs. The cells not treated with Bgn-SeNPs were considered as control. The 12-well plates were shaken gradually after 24 hrs of Bgn-SeNPs' exposure to homogenize the released lactate dehydrogenase (LDH) in the cell culture medium, and the medium was transferred to 1.5 mL sterilized centrifuge tubes and centrifuged at 12,000 rpm for 15 min under 4 °C to separate cellular debris and Bgn-SeNPs. Following, 100 µL of cell-free supernatant was added to the substrate solution and the absorbance at 340 nm was measured with a microplate reader (Synergy H1, BioTek, USA). The LDH activity of the Bgn-SeNPs was determined by measuring the rate of decrease in NADH absorbance over time (slopes). The results of the study were expressed with respect to control (%) (Han et al., 2011).

2.5.3.3 Micro-morphological observation

Briefly, 50,000 cells were seeded in cell culture dishes in a DMEM medium, which was free from FBS and allowed to adhere for 8 hrs. Following, cells were treated with Bgn-SeNPs for 24 hrs. The images of the cells were captured using an inverted microscope (Olympus, Japan) and the micro-morphology of cells was considered to evaluate the inhibitory activity of Bgn-SeNPs (Swaminathan et al., 2019). The cisplatin was used as a standard anticancer agent.

2.6 Statistical analysis

The assays were carried out in triplicates (n = 3) and obtained results were expressed as mean ± standard deviation. The obtained data were analyzed by one-way ANOVA and statistical analysis was done by student's t-test. The analysis and graphical representation were done using GraphPad Prism free trial version 7, USA.

III. Results and discussion

3.1 Biogenic synthesis and physico-chemical characterization of Bgn-SeNPs

The present study aimed to synthesize biogenic selenium nanoparticles (Bgn-SeNPs) utilizing the reducing and stabilizing potentials of *Vaccinium* sect. *Cyanococcus* fruit extract. In the present study, the color of the reaction solution (sodium selenite solution with *Vaccinium* sect. *Cyanococcus* fruit extract) was changed after 3 hrs of the incubation period and showed the formation of biogenic selenium nanoparticles (Bgn-SeNPs). A significant color change from pale yellow to brick red was noted after 3 days of the incubation period (Vundela et al., 2022). Following, as-synthesized Bgn-SeNPs were subjected to various physico-chemical characterization analyses.

Utilizing the concept of plasmon resonance, UV-Visible spectroscopy was used to establish the initial confirmation of Bgn-SeNPs synthesis and an absorption peak was noticed at 320 nm (**Fig. 1**). In support of our study, previous researchers utilized plant materials for the conversion of sodium selenite into Bgn-SeNPs. Menon et al., (2019) synthesized Bgn-SeNPs from the extract of ginger and showed characteristic UV-Visible peaks at 370 and 420 nm which is representative of surface plasmon resonance (SPR) for SeNPs. Similarly, Kokila et al., (2017) synthesized Bgn-SeNPs from *Diospyros montana* leaf extract and showed a characteristic UV-Visible peak at 261 nm. The previous researchers concluded that the characteristic UV-Visible peak is due to SPR. The obtained UV-Visible spectroscopy revealed that the sodium selenite has been successfully converted to Bgn-SeNPs by the reduction and stabilization action of *Vaccinium* sect. *Cyanococcus* fruit extract.

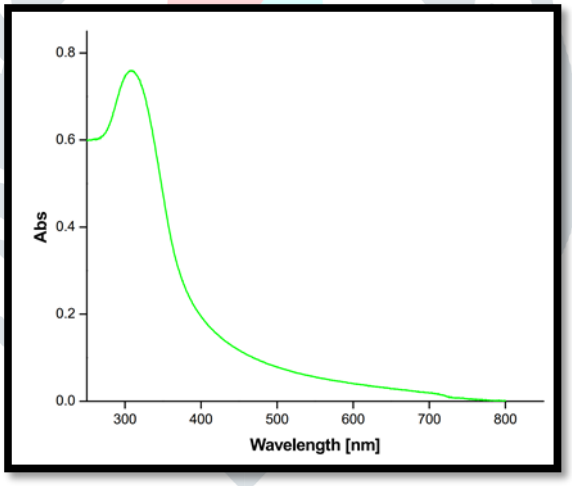

Figure 1: UV-Visible spectrum of biogenic selenium nanoparticles (Bgn-SeNPs).

An X-ray diffractometer (XRD) was used to determine the phase of Bgn-SeNPs. In our study, the XRD pattern of Bgn-SeNPs showed broader peaks and sharp peaks were absent (**Fig. 2**). The results showed that Bgn-SeNPs was not exhibited crystalline nature and were found to have amorphous in nature. According to our results, Gunti et al., (2019) synthesized Bgn-SeNPs from *Emblica officinalis* fruit extract and described it as amorphous particularly shapeless. The study concludes that Bgn-SeNPs were amorphous due to the selenium atoms' uneven arrangement and unorganized chain shape (Li et al., 2007).

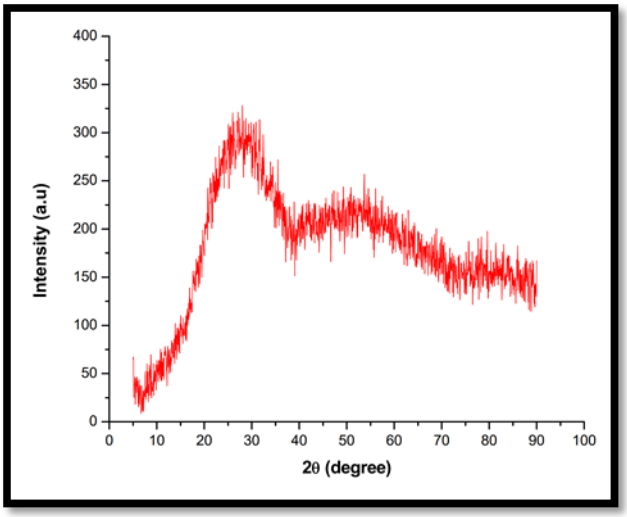

Figure 2: X-ray diffractometer (XRD) pattern of biogenic selenium nanoparticles

The dynamic light scattering (DLS) pattern of Bgn-SeNPs was is carried out to know the dynamic size in dispersion solution. According to our study's DLS pattern, synthesized Bgn-SeNPs were nanosized, with an average size of 130 nm (**Fig. 3**). The DLS analysis also found that the absence of multiple peaks indicated that Bgn-SeNPs were monodispersed. The polydispersity index for Bgn-SeNPs that we observed was < 0.23, indicating that Bgn-SeNPs were discovered in a less aggregative form. According to our results, Menon et al., (2019) synthesized Bgn-SeNPs from plant sources and discovered that the dynamic size of Bgn-SeNPs is 100 – 120 nm. The study concluded that Bgn-SeNPs were nanosized in dispersion form.

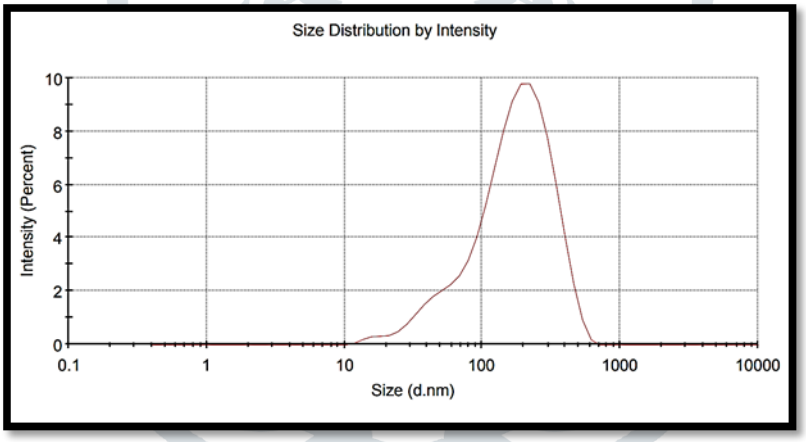

Figure 3: Dynamic light scattering (DLS) pattern of biogenic selenium nanoparticles.

To determine the effective electric charge on the surface, the zeta potential of Bgn-SeNPs is measured. The stability of the nanomaterial is determined by its zeta potential, which is absolutely necessary for the material to endure and function properly. Higher electrical repulsion between the materials causes them to have a tendency toward improved stability. In our study, Bgn-SeNPs has found negative in charge and exhibited a zeta potential of -25 mV (**Fig. 4**). The polyphenols present in the VC fruit extract may be the cause of the negative charge on Bgn-SeNPs. The Bgn-SeNPs in dispersion form favor to be the existence of negative electrostatic forces. In support of our study, Menon et al., (2019) synthesized Bgn-SeNPs from plant sources and discovered the zeta potential of Bgn-SeNPs as -36 mV. The study concluded that Bgn-SeNPs were negative in charge.

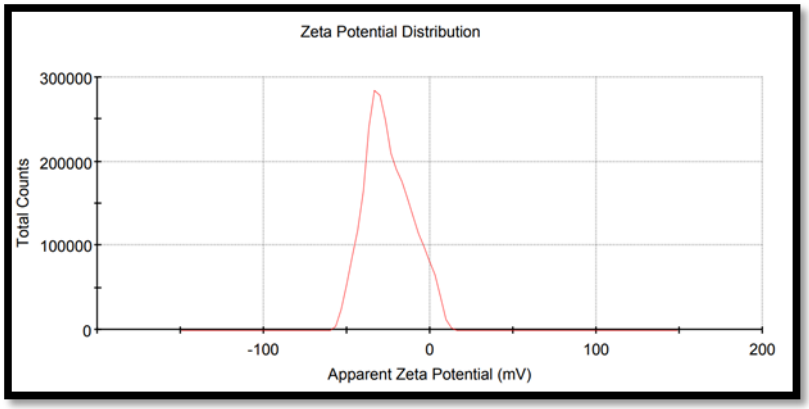

Figure 4: Zeta potential distribution of biogenic selenium nanoparticles.

The Figure 5 displayed the Bgn-SeNPs SEM observation. The Bgn-SeNPs were identified as having an irregular shape, a slight aggregation, and sizes between 106 – 150 nm. In support of our results, Gunti et al., (2019), Menon et al., (2019), and Kokila et al., (2017) have reported that Bgn-SeNPs from plant extracts were slightly agglomerated and it could be due to chemical constituents of VC fruit extract.

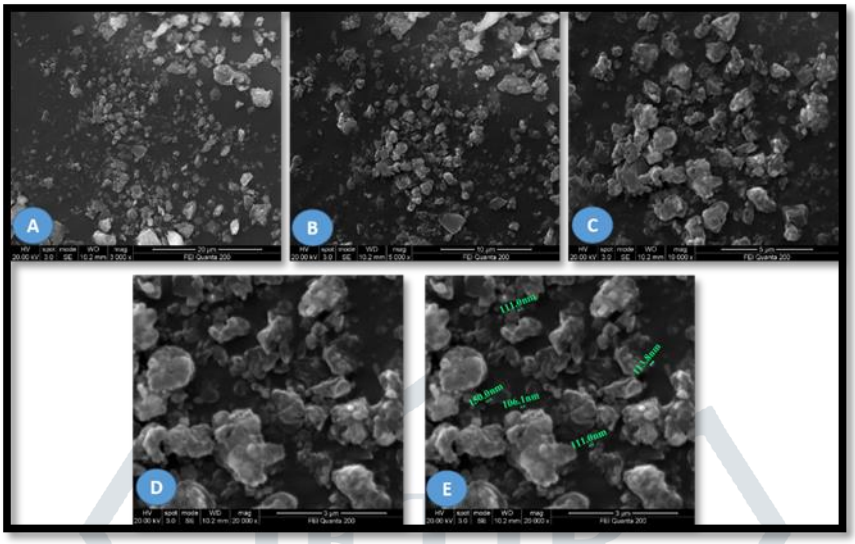

Figure 5: Scanning electron microscopic images of biogenic selenium nanoparticles (Bgn-SeNPs). (A) Bgn-SeNPs at 3,000 x. (B) Bgn-SeNPs at 5,000 x. (C) Bgn-SeNPs at 10,000 x. (D) Bgn-SeNPs at 20,000 x. (E) Bgn-SeNPs at 20,000 x marked with size.

3.2 Anticancer activity of Bgn-SeNPs

3.2.1 Cell viability analysis

Anticancer activity of Bgn-SeNPs was performed on various cancer cell line models, which include RAW 264.7 (mouse macrophage cells), A549 (human lung cancer cells), MDA-MB-231 (human breast cancer cells), and Caco-2 (human intestinal cancer cells). The biocompatibility of Bgn-SeNPs was evaluated by the accomplishment of the cytotoxicity analysis on human normal kidney cells HEK-293. The inhibitory effect of Bgn-SeNPs on cell viability of cancer and normal cells was assessed by cell viability assays such as MTT, LDH, and micro-morphological observation.

3.2.1.1 MTT assay

The evaluation of cytotoxic medication therapy has been carried out most frequently using the MTT assay. The MTT procedure can be implemented more easily in cell cultures grown in suspension, hence the assay has been investigated for its potential to be used as a predictor when choosing a leukemia treatment regimen. The assays are highly accurate at predicting both drug sensitivity and drug resistance. The cellular reduction of tetrazolium salts to their formazan crystal forms is the foundation of the MTT assay. It is important to identify the cell concentration range where the optical density and the total number of counted cells are directly correlated. The MTT assay's benefits include simplicity and speed of execution, repeatability of results, and clinical correlation between in-vitro and in-vivo analysis (Freimoser et al., 1999).

In the present study, Bgn-SeNPs have dose-dependently inhibited the cell viability of cancer cells and normal cells (**Fig. 6 A & B**). The Bgn-SeNPs have exhibited superior anticancer activity on A549 (human lung cancer cells) and are followed by Caco-2 (human intestinal cancer cells). The lowest anticancer activity was noticed against MDA-MB-231 (human breast cancer cells). The IC_{50} values of Bgn-SeNPs (concentration required to inhibit 50% of cell viability) on RAW 264.7, A549, MDA-MB-231, and Caco-2 cancer cells were determined as 64.29 ± 3.71, 38.03 ± 2.14, 67.81 ± 3.05, and 54.73 ± 2.90 µg/mL, respectively. The IC_{50} values of cisplatin on RAW 264.7, A549, MDA-MB-231, and Caco-2 cancer cells were determined as 3.41 ± 0.09, 3.09 ± 0.07, 3.94 ± 0.03, and 2.74 ± 0.02 µM, respectively.

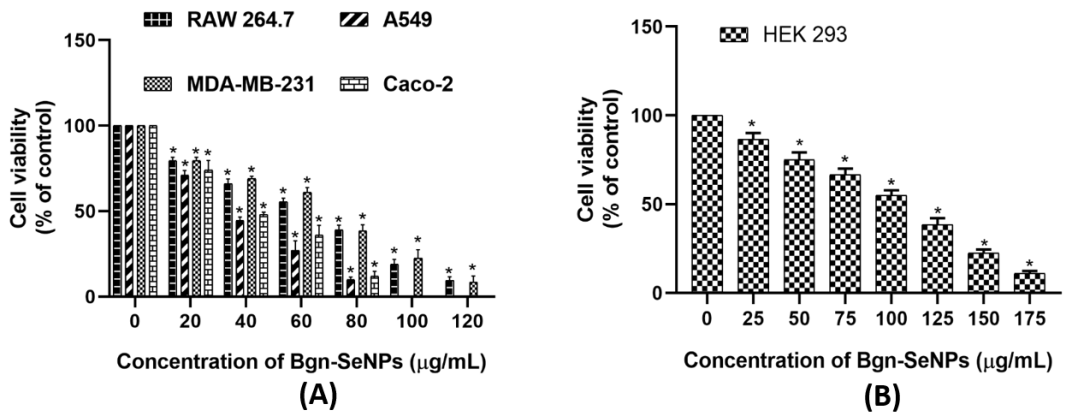

Figure 6: (A) Anticancer effect of Bgn-SeNPs on cell viability of cancer cells determined by MTT assay. **(B)** Cytotoxic effect of Bgn-SeNPs on cell viability of human normal kidney cells HEK-293 determined by MTT assay. The analysis was carried out in triplicates (n = 3) and the results were expressed as mean ± standard deviation. The statistical significance between the control and test samples within the respective analysis was determined by Dunnett's test and a *p*-value ≤ 0.05 was considered significant. The symbol '#' denotes that the test sample is not significant with respect to control. Whereas the symbol '*' denotes that the test sample is significant with respect to control.

The cytotoxicity/biocompatibility of Bgn-SeNPs on human normal kidney cells HEK-293 was assessed by MTT assay. The Bgn-SeNPs have dose-dependently inhibited the growth of the normal cells. However, the concentration of Bgn-SeNPs required to inhibit the growth of the human normal kidney cells HEK-293 was found quite high compared to cancer cells RAW 264.7, A549, MDA-MB-231, and Caco-2 cells. The IC_{50} value of Bgn-SeNPs (concentration required to inhibit 50% of cell viability) on HEK-293 cells was determined as 110.29 ± 5.94 µg/mL. Whereas, the IC_{50} value of cisplatin on HEK-293 cells was determined as 5.41 ± 0.81 µM. The concentration of cisplatin required to inhibit the growth of cancer cells was found much lower compared to normal cells, which indicated that the standard anticancer drug cisplatin is highly selective towards cancer cells. Similarly, Bgn-SeNPs are less cytotoxic toward normal cells compared to cancer cells, which shows that Bgn-SeNPs are highly biocompatible. In accordance with our study, Vundela et al., (2022) biosynthesized Bgn-SeNPs from *C. papaya* fruit extract and demonstrated their selective anticancer activity in RAW 264.7, Caco-2, MCF-7, and IMR-32 by comparing with normal cell line Vero by MTT assay. The study concluded that as-synthesized Bgn-SeNPs were highly selective in inhibiting the cancer cells in relation to normal cells.

3.2.1.2 LDH assay

Cytotoxicity LDH assay measures the amount of lactate dehydrogenase (LDH) activity secreted by injured cells to assess cytotoxicity. All cell types include the stable cytoplasmic enzyme LDH, which is released into the media for cell culture through broken plasma membranes. A soluble cytosolic enzyme is LDH that is rapidly liberated into the extracellular environment after cellular membrane disruption caused by apoptosis or necrosis, and hence acts as an indication of lytic cell death. Even though it is commonly recognized as a marker of cell death. When LDH converted pyruvate to lactate, the assay was designed to measure the oxidation of β-NADH to β-NAD^+, which was quantified as a change in absorbance at 340 nm. An aliquot of cell culture medium combines with a tetrazolium salt, which is transformed to a red formazan end product by NADH produced by LDH release and read on a spectrophotometer (Jurisic et al., 2015).

In the present study, Bgn-SeNPs dose-dependently increased the LDH release in both cancer and normal cells (**Fig. 7 A & B**). However, superior LDH release was noticed in cancer cells at lower concentrations of Bgn-SeNPs. Whereas, Bgn-SeNPs induced the LDH release in normal at a higher dosage. The study showed that Bgn-SeNPs have selectively induced cell membrane damage at a lower dose in cancer cells related to normal cells. In support of our study, Vundela et al., (2022) biosynthesized Bgn-SeNPs from *C. papaya* fruit extract and demonstrated their selective anticancer activity in RAW 264.7, Caco-2, MCF-7, and IMR-32 by comparing with normal cell line Vero by LDH assay. The study concluded that as-synthesized Bgn-SeNPs were highly selective in inhibiting the cancer cells in relation to normal cells through damaging/disturbing the cell membrane.

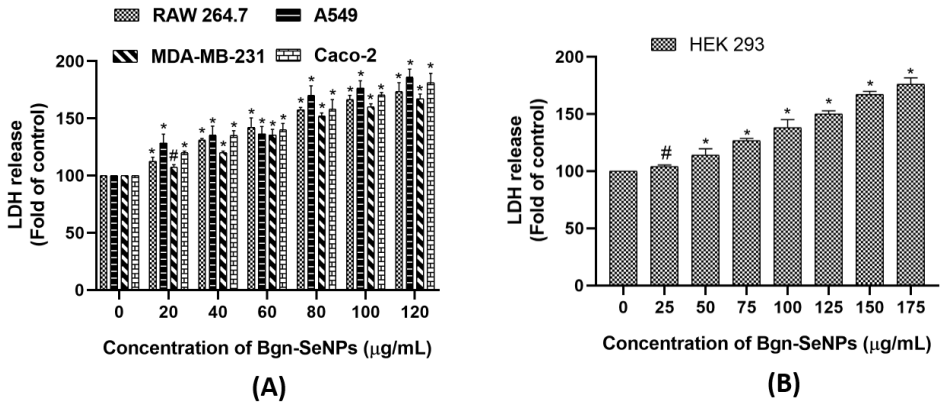

Figure 7: Effect of Bgn-SeNPs on cell viability of cancer cells and normal cells determined by LDH assay. **(A)** Dose-dependent effect of Bgn-SeNPs on LDH release in cancer cells. **(B)** Dose-dependent effect of Bgn-SeNPs on LDH release in normal cells. The analysis was carried out in triplicates (n = 3) and the results were expressed as mean ± standard deviation. The statistical significance between the control and test samples within the respective analysis was determined by Dunnett's test and a *p*-value ≤ 0.05 was considered significant. The symbol '#' denotes that the test sample is not significant with respect to control. Whereas the symbol '*' denotes that the test sample is significant with respect to control.

3.2.1.3 Micro-morphological observation

The anticancer and cytotoxic effect of Bgn-SeNPs on cancer and normal cells were revealed by micro-morphological observation, which was done by capturing cellular images under bright-field microscopic images. The micro-morphology of control and cells treated with IC_{50} values of Bgn-SeNPs and cisplatin were shown in **Figures 8, 9, & 10**. In both cancer and normal cells, control cells showed smooth and monolayer during bright-field microscopic analysis, indicating that the cells were healthy. The cells treated with IC_{50} values of Bgn-SeNPs and cisplatin clearly displayed cellular membrane disruption, leaking of cellular debris, and development of apoptotic bodies. However, the dose of Bgn-SeNPs and cisplatin required to induce detrimental changes in the micro-morphology of normal was quite higher related to cancer cells. The observed micro-morphological features were in line with the results of MTT and LDH assays. The study concluded that Bgn-SeNPs selectively show the growth inhibitory activity on cancer cells. The concentration of Bgn-SeNPs required to induce cytotoxicity in normal cells was quite higher than in related cancer cells and therefore, Bgn-SeNPs could be considered highly biocompatible toward normal cells. The overall cell viability studies showed that Bgn-SeNPs have potential anticancer activity and superior anticancer activity was observed in A549 cells.

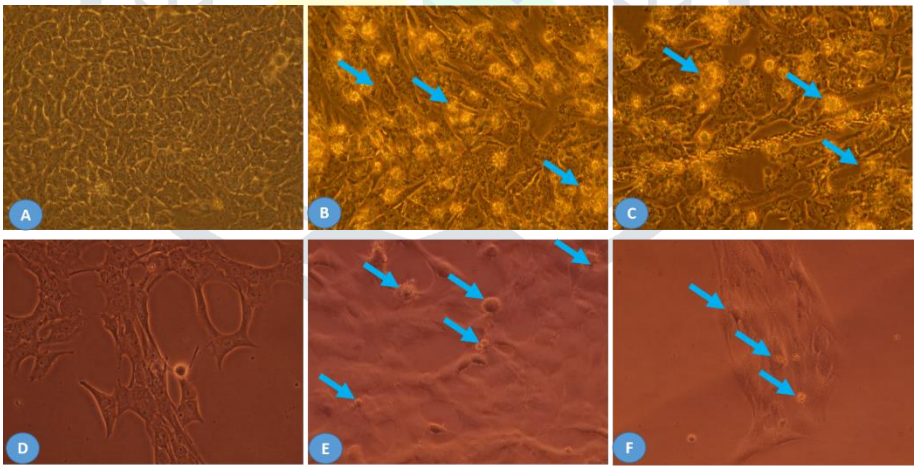

Figure 8: Effect of biosynthesized selenium nanoparticles (Bgn-SeNPs) and cisplatin on micro-morphology of A549 and MDA-MB-231 cancer cells observed by bright-field microscope. (**A)** A549 control cells. (**B)** A549 cells treated with IC_{50} value of Bgn-SeNPs (38.03 ± 2.14 µg/mL). **(C)** A549 cells treated with IC_{50} value of cisplatin (3.09 ± 0.07 µM). **(D)** MDA-MB-231 control cells. **(E)** MDA-MB-231 cells treated with IC_{50} value of Bgn-SeNPs (67.81 ± 3.05 µg/mL). **(F)** MDA-MB-231 cells treated with IC_{50} value of cisplatin (3.94 ± 0.03 µM). The images were displayed at a magnification of 400x.

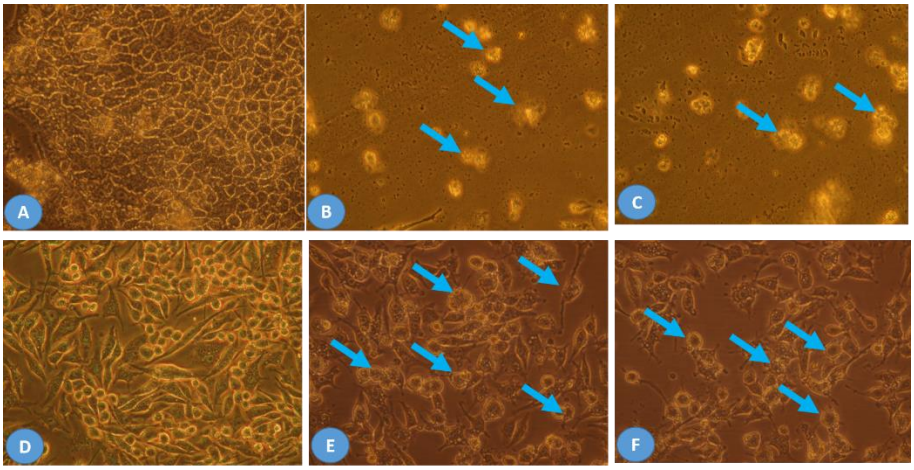

Figure 9: Effect of biosynthesized selenium nanoparticles (Bgn-SeNPs) and cisplatin on micro-morphology of Caco-2 and RAW 264.7 cancer cells observed by bright-field microscope. (**A)** Caco-2 control cells. (**B)** Caco-2 cells treated with IC_{50} value of Bgn-SeNPs (54.73 ± 2.90 µg/mL). **(C)** Caco-2 cells treated with IC_{50} value of cisplatin (2.74 ± 0.02 µM). **(D)** RAW 264.7 control cells. **(E)** RAW 264.7 cells treated with IC_{50} value of Bgn-SeNPs (64.29 ± 3.71 µg/mL). **(F)** RAW 264.7 cells were treated with IC_{50} value of cisplatin (3.41 ± 0.09 µM). The images were displayed at a magnification of 400x.

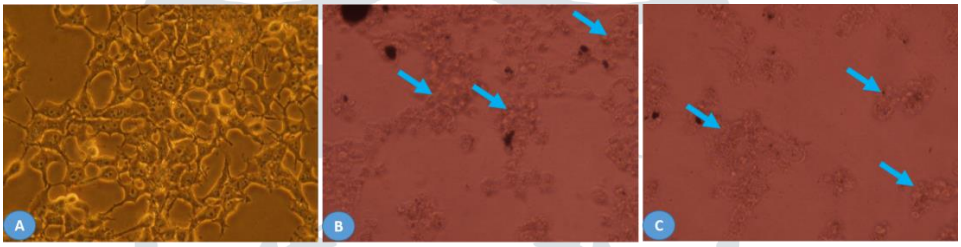

Figure 10: Effect of biosynthesized selenium nanoparticles (Bgn-SeNPs) and cisplatin on micro-morphology of HEK 293 normal cells observed by bright-field microscope. (**A)** HEK 293 control cells. (**B)** HEK 293 cells treated with IC_{50} value of Bgn-SeNPs (110.29 ± 5.94 µg/mL). **(C)** HEK 293 cells treated with IC_{50} value of cisplatin (5.41 ± 0.81 µM). The images were displayed at a magnification of 400x.

IV. Conclusion

In the study, biogenic selenium nanoparticles were successfully synthesized from *Vaccinium* sect. *Cyanococcus* fruit extract. The as-synthesized Bgn-SeNPs were amorphous in nature, highly stable with a negative charge, and found in nano-sized. The as-synthesized Bgn-SeNPs potential inhibited the growth of RAW 264.7, A549, MDA-MB-231, and Caco-2 cancer cells and exhibited potential anticancer activity. Interestingly, a dose of Bgn-SeNPs required to induce cell death in normal cells was quite higher related to cancer cells. The study concluded that as-synthesized Bgn-SeNPs were highly selective in inhibiting cancer cells in relation to normal cells. The as-synthesized Bgn-SeNPs could be highly applicable in the biomedical field as an anticancer agent. However, an in-detailed anticancer mechanism and safety assessment of Bgn-SeNPs are needed for further conclusion.

V. Acknowledgment

Authors were thankful to Acharya Nagarjuna Unviversity for providing the facility and support.

REFERENCES

[1]. Akram, M., Munir, N., Daniyal, M., Egbuna, C., Găman, M.A., Onyekere, P.F., and Olatunde, A. 2020. Vitamins and Minerals: Types, sources and their functions. In Functional Foods and Nutraceuticals. Springer, Cham: 149-172.

[2]. Alvi, G. B., Iqbal, M. S., Ghaith, M. M. S., Haseeb, A., Ahmed, B., and Qadir, M. I. 2021. Biogenic selenium nanoparticles (SeNPs) from citrus fruit have anti-bacterial activities. Scientific Reports, 11(1): 1-11.

[3]. Freimoser, F.M., Jakob, C.A., Aebi, M., and Tuor, U. 1999. The MTT [3-(4, 5-dimethylthiazol-2-yl)-2, 5-diphenyltetrazolium bromide] assay is a fast and reliable method for colorimetric determination of fungal cell densities. Applied and environmental microbiology, 65(8): 3727-3729.

[4]. Gunti, L., Dass, R.S., and Kalagatur, N.K. 2019. Phytofabrication of selenium nanoparticles from *Emblica officinalis* fruit extract and exploring its biopotential applications: antioxidant, antimicrobial, and biocompatibility. Frontiers in microbiology, 10: 931.

[5]. Habeeb Rahuman, H.B., Dhandapani, R., Narayanan, S., Palanivel, V., Paramasivam, R., Subbarayalu, R., ... and Muthupandian, S. 2022. Medicinal plants mediated the green synthesis of silver nanoparticles and their biomedical applications. IET nanobiotechnology, 16(4): 115-144.

[6]. Han, X., Gelein, R., Corson, N., Wade-Mercer, P., Jiang, J., Biswas, P., Jacob N. Finkelstein, J.N., Elder, A., & Oberdorster, G. 2011. Validation of an LDH assay for assessing nanoparticle toxicity. Toxicology, 287(1-3): 99-104.

[7]. He, Y., Xiang, Y., Zhou, Y., Yang, Y., Zhang, J., Huang, H., ... and Tang, L. 2018. Selenium contamination, consequences and remediation techniques in water and soils: A review. Environmental Research, 164: 288-301.

[8]. Ikram, M., Javed, B., and Raja, N.I. 2021. Biomedical potential of plant-based selenium nanoparticles: a comprehensive review on therapeutic and mechanistic aspects. International Journal of Nanomedicine, 16: 249–268.

[9]. Jurisic, V., Radenkovic, S., and Konjevic, G. 2015. The actual role of LDH as tumor marker, biochemical and clinical aspects. Advances in Cancer Biomarkers, 867: 115-124.

[10]. Khanna, P.K., Bisht, N., and Phalswal, P. 2022. Selenium nanoparticles: a review on synthesis and biomedical applications. Materials Advances, 3: 1415-1431

[11]. Kokila, K., Elavarasan, N., and Sujatha, V. 2017. *Diospyros montana* leaf extract-mediated synthesis of selenium nanoparticles and their biological applications. New Journal of Chemistry, 41(15): 7481-7490.

[12]. Koshovets, O.B. and Ganichev, N.A. 2017. Nanotechnology and the new technological revolution: Expectations and reality. Studies on Russian Economic Development, 28(4): 391-397.

[13]. Li, S., Shen, Y., Xie, A., Yu, X., Zhang, X., Yang, L., and Li, C. 2007. Rapid, room-temperature synthesis of amorphous selenium/protein composites using *Capsicum annuum* L extract. Nanotechnology, 18(40): 405101.

[14]. Menon, S., Shrudhi Devi, .K.S, Agarwal, H., and Shanmugam, V. K. 2019. Efficacy of biogenic selenium nanoparticles from an extract of ginger towards evaluation on anti-microbial and anti-oxidant activities. Colloid and Interface Science Communications, 29: 1-8.

[15]. Roduner, E. 2006. Size matters: why nanomaterials are different. Chemical Society Reviews, 35(7): 583-592.

[16]. Swaminathan, S., Haribabu, J., Kalagatur, N. K., Konakanchi, R., Balakrishnan, N., Bhuvanesh, N., and Karvembu, R. 2019. Synthesis and anticancer activity of [RuCl2 (η6-arene)(aroylthiourea)] complexes—high activity against the human neuroblastoma (IMR-32) cancer cell line. ACS omega, 4(4): 6245-6256.

[17]. Vundela, S. R., Kalagatur, N. K., Nagaraj, A., Kadirvelu, K., Chandranayaka, S., Kondapalli, K., ... & Poda, S. 2022. Multi-biofunctional properties of phytofabricated selenium nanoparticles from *Carica papaya* fruit extract: Antioxidant, antimicrobial, antimycotoxin, anticancer, and biocompatibility. Frontiers in microbiology, 12: 769891

[18]. Wadhwani, S.A., Shedbalkar, U.U., Singh, R., & Chopade, B.A. 2016. Biogenic selenium nanoparticles: current status and future prospects. Applied microbiology and biotechnology, 100(6): 2555-2566.

[19]. Yaqoob, A.A., Ahmad, H., Parveen, T., Ahmad, A., Oves, M., Ismail, I.M., ... and Mohamad Ibrahim, M.N. 2020. Recent advances in metal decorated nanomaterials and their various biological applications: a review. Frontiers in chemistry, 8: 341.